




Nasal Tissue Extraction Is Essential for Characterization of the Murine Upper Respiratory Tract Microbiota

L. Patrick Schenck,^{a,b,c,d} Joshua J. C. McGrath,^d Daphnée Lamarche,^{a,b,c} Martin R. Stämpfli,^{d,e,f,g}  Dawn M. E. Bowdish,^{c,d,f}
 Michael G. Surette^{b,c,g}

^aDepartment of Biochemistry and Biomedical Sciences, McMaster University, Hamilton, Ontario, Canada

^bFarncombe Family Digestive Health Research Institute, McMaster University, Hamilton, Ontario, Canada

^cMichael G. Degroote Institute for Infectious Disease Research, McMaster University, Hamilton, Ontario, Canada

^dMcMaster Immunology Research Centre, McMaster University, Hamilton, Ontario, Canada

^eFirestone Institute for Respiratory Health, McMaster University, Hamilton, Ontario, Canada

^fDepartment of Pathology and Molecular Medicine, McMaster University, Hamilton, Ontario, Canada

^gDepartment of Medicine, McMaster University, Hamilton, Ontario, Canada

ABSTRACT Respiratory infections are a leading cause of morbidity and mortality worldwide. Bacterial pathogens often colonize the upper respiratory tract (nose or mouth) prior to causing lower respiratory infections or invasive disease. Interactions within the upper respiratory tract between colonizing bacteria and the resident microbiota could contribute to colonization success and subsequent transmission. Human carriage studies have identified associations between pathogens such as *Streptococcus pneumoniae* and members of the resident microbiota, although few mechanisms of competition and cooperation have been identified and would be aided by the use of animal models. Little is known about the composition of the murine nasal microbiota; thus, we set out to improve assessment, including tissue sampling, composition, and comparison between mouse sources. Nasal washes were efficient in sampling the nasopharyngeal space but barely disrupted the nasal turbinates. Nasal tissue extraction increased the yield of cultivable bacterial compared to nasal washes, revealing distinct community compositions. Experimental pneumococcal colonization led to dominance by the colonizing pathogen in the nasopharynx and nasal turbinates, but the composition of the microbiota, and interactions with resident microbes, differed depending on the sampling method. Importantly, vendor source has a large impact on microbial composition. Bacterial interactions, including cooperation and colonization resistance, depend on the biogeography of the nose and should be considered during research design of experimental colonization with pathogens.

IMPORTANCE The nasal microbiota is composed of species that play a role in the colonization success of pathogens, including *Streptococcus pneumoniae* and *Staphylococcus aureus*. Murine models provide the ability to explore disease pathogenesis, but little is known about the natural murine nasal microbiota. This study established techniques to allow the exploration of the bacterial members of the nasal microbiota. The mouse nasal microbiota included traditional respiratory bacteria, including *Streptococcus*, *Staphylococcus*, and *Moraxella* species. Analyses were affected by different sampling methods as well as the commercial source of the mice, which should be included in future research design of infectious disease research.

KEYWORDS *Streptococcus pneumoniae*, colonization, microbiota, upper respiratory tract

The upper respiratory tract (URT) is the initial barrier against airway pathogens. Asymptomatic colonization by potential pathogens, including *Streptococcus pneumoniae* and *Staphylococcus aureus*, provides a reservoir capable of causing disease

Citation Schenck LP, McGrath JJC, Lamarche D, Stämpfli MR, Bowdish DME, Surette MG. 2020. Nasal tissue extraction is essential for characterization of the murine upper respiratory tract microbiota. *mSphere* 5:e00562-20. <https://doi.org/10.1128/mSphere.00562-20>.

Editor Vincent B. Young, University of Michigan—Ann Arbor

Copyright © 2020 Schenck et al. This is an open-access article distributed under the terms of the [Creative Commons Attribution 4.0 International license](https://creativecommons.org/licenses/by/4.0/).

Address correspondence to Dawn M. E. Bowdish, bowdish@mcmaster.ca.

Received 11 June 2020

Accepted 11 November 2020

Published 16 December 2020

within the host or being transmitted to other carriers via respiratory droplets (1). Pathogens could inhibit colonization by other pathogens, as epidemiological studies have identified a negative correlation between *S. pneumoniae* and *S. aureus* in children (2, 3). Consistent with this, studies of pneumococcal vaccination have shown that the removal or reduction of *S. pneumoniae* is associated with increased *S. aureus* colonization (4). The contribution of the resident microbiota is relatively unknown, although a recent study demonstrated that a nasopharyngeal bacterial composition with high levels of *Corynebacterium* or *Dolosigranulum* species was correlated with a reduced risk of lower respiratory infections (5). The antipathogenic activities of *Corynebacterium* species have been identified *in vitro* (6, 7). A further understanding of the agonistic and antagonistic interactions between microbial species may explain why certain populations are more susceptible to colonization and infection.

Mechanistic studies involving pneumococcal colonization and the URT microbiota are difficult due to high interindividual variability, low bacterial biomass, and diverse topography. An experimental human pneumococcal colonization model identified increased α -diversity (higher microbial community diversity within a subject) in subjects with successful pneumococcal colonization (8). Identification of the contribution of individual bacterial species was challenging due to distinct microbial compositions between subjects. Mouse models allow for greater control over microbial composition and have been used to assess the alterations of the nasal microbiota during pneumococcal infection (9, 10); however, little is known about the naive URT microbiota composition in mice.

Assessment of murine nasal bacteria is predominated by nasal washes. Cannulation and flushing from trachea to nares, often called a nasal wash, are the most frequently used methods to assess nasal colonization, although tissue extraction is sometimes used to assess adherent or invasive pathogens (11–14). Differences in the duration of colonization and bacterial interactions have been identified using different tissue extraction methods (14–17). No studies have compared these two sampling methods for their efficiency at extracting the native microbiota and their impact on pathogen-microbiota associations. We used culture-dependent and -independent methods to assess the composition of the URT microbiota using nasal washes and complete tissue collection. Nasal washes were sufficient for sampling the nasopharynx but did not disrupt the turbinates. Nasal tissue collection yielded a distinct community with increased bacterial loads compared to those in nasal wash samples. We show that nasal wash may underestimate the presence and interactions of *Streptococcus pneumoniae* within the URT. Furthermore, the URT microbiota composition differs by the source of the mice. This approach to microbial analysis of the murine URT will improve the study design of host-pathogen and pathogen-commensal interactions during colonization.

RESULTS

Nasal wash does not completely disrupt nasal surfaces. The biogeography affected by a nasal wash is unknown. We performed nasal washes using a gentle buffer (phosphate-buffered saline [PBS]) or a harsh buffer (buffer RLT), followed by histological assessment of the nasal tissue via hematoxylin-and-eosin staining (Fig. 1A and B). PBS does not affect the epithelial architecture of the nasal cavity (Fig. 1C to E), whereas buffer RLT disrupts the epithelial layer within the nasopharyngeal space and septum as well as the nasal-associated lymphoid tissue (Fig. 1G and H) but not the nasal turbinates (Fig. 1F). Overall, nasal washes with harsh buffers were unable to disrupt a large majority of the epithelial layer in the nasal cavity, implying that nasal washes do not accurately sample the complete biogeography of the nasal tissue (Fig. 1A and B).

Nasal tissue extraction recovers more bacteria than nasal washes. Nasal wash and nasal tissue samples were homogenized, plated on brain heart infusion (BHI) agar and fastidious anaerobic agar (FAA), and incubated aerobically and anaerobically, respectively. Overall, the bacterial load was low in both complete nasal tissue (cNT) and nasal wash samples ($\sim 10^3$ CFU/mouse). Nasal tissue had significantly higher bacterial loads and diversity of colony morphotypes than nasal wash samples (Fig. 2A). Complementary

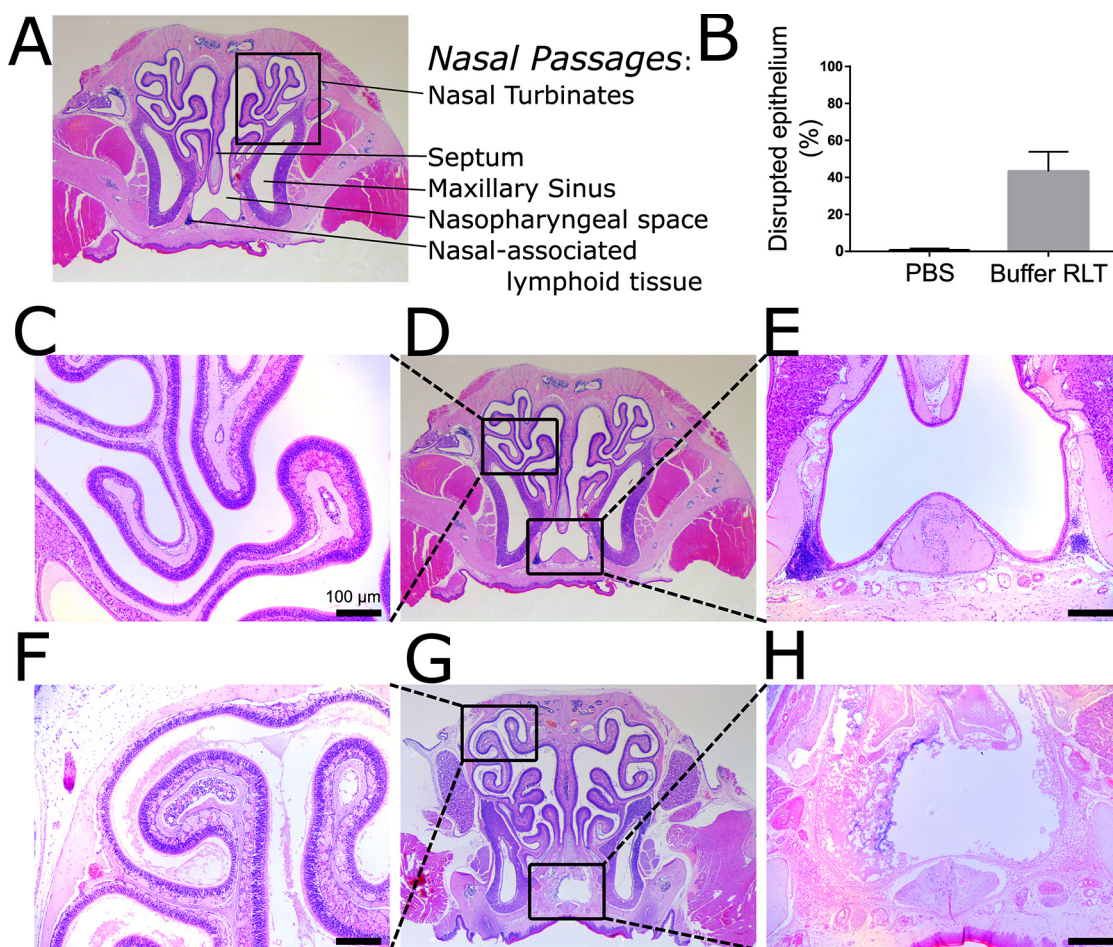


FIG 1 Nasal wash does not effectively sample the nasal cavity. (A) Nasal cavities were washed with PBS ($n=3$) and buffer RLT ($n=3$), and tissues were collected for histological analysis. (B) Hematoxylin-and-eosin-stained cross sections demonstrate that nasal washes with PBS do not disrupt the epithelial layer compared to buffer RLT. (C to E) Specifically, PBS washes do not impact the epithelial architecture in the turbinates (C and D) or the nasopharyngeal space (E). (F to H) Buffer RLT washes greatly disrupt the nasopharyngeal space (G and H) but not the nasal turbinates (F).

to culture-based analysis, 16S rRNA gene sequencing revealed that cNT and nasal wash samples clustered separately from each other (Fig. 2B) ($P < 0.05$ by permutational multivariate analysis of variance [PERMANOVA]; $R^2 = 0.181$). *Streptococcus* species and *Staphylococcus* species were dominant in nasal tissue and wash samples (Fig. 2C). This difference in microbial composition was driven by nasal tissue containing significantly more *Neisseriaceae*, *Actinomyces*, and *Bifidobacterium* species, while nasal wash samples contained more *Erysipelotrichaceae* and *Cyanobacteria* (Fig. 2D) (linear discriminant analysis [LDA] effect size [LEfSe]). No difference was seen in Shannon diversity ($P=0.26$) or observed species ($P=0.4181$) between nasal wash and nasal tissue samples (see Fig. S1 in the supplemental material).

The mouse nasal microbiota is distinct from the gut microbiota. It has been reported that a significant amount of the bacterial DNA found in the URT is from environmental contamination rather than being due to resident microbes (18). In mice, contaminating DNA can come from exposure to fecal matter and/or reagent controls. To determine the degree to which microbial profiles are influenced by fecal exposure, we compared the nasal tissue and gut microbiota within a mouse. The nasal microbiota was distinct from the gut microbiota (Fig. S2A) ($P < 0.001$ by PERMANOVA; $R^2 = 0.383$). The gut microbiota has greatly increased α -diversity compared to the nasal microbiota (Fig. S2B). Additionally, the dominant families in the gut (*Muribaculaceae*, *Lactobacillaceae*, *Lachnospiraceae*, and *Erysipelotrichaceae*) are different from the

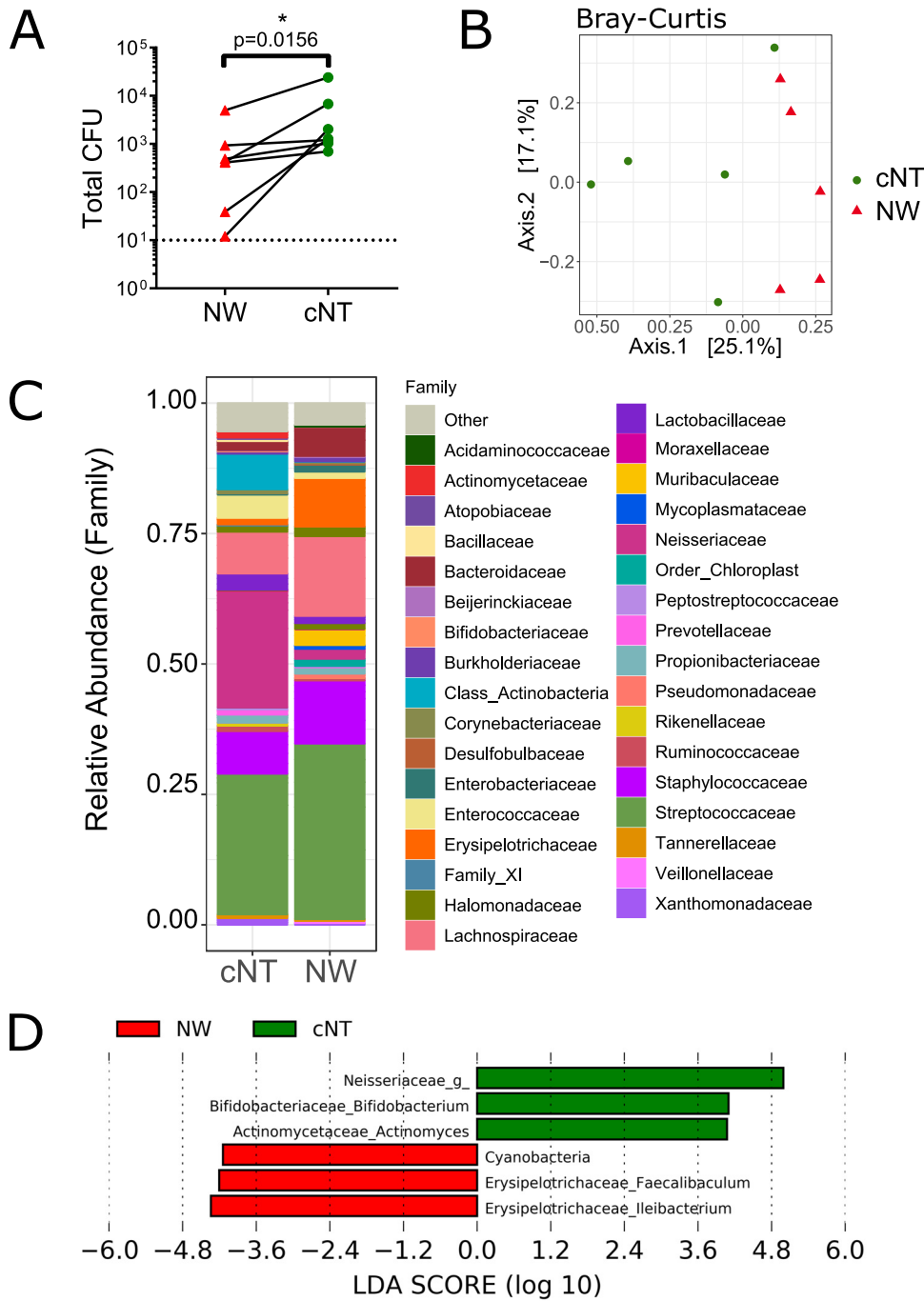


FIG 2 Nasal tissue extraction is essential for complete microbiota assessment. Nasal wash samples were collected using PBS, followed by tissue collection from the same mice and V3 16S rRNA gene high-throughput sequencing. (A) Nasal tissue had significantly more bacteria than nasal wash (NW) samples. (B) Nasal tissue microbial communities clustered separately from nasal wash communities ($P < 0.05$ by Bray-Curtis PERMANOVA). (C and D) Nasal tissue microbiota were enriched in *Neisseriaceae*, *Bifidobacterium*, and *Actinomyces*, while nasal wash samples were enriched in *Erysipelotrichaceae* and *Cyanobacteria* (LEfSe).

dominant families in the nasal tissue (*Streptococcaceae*, *Staphylococcaceae*, and *Enterococcaceae*) microbiota (Fig. S2C).

The mouse nasal microbiota is distinct from extraction and sequencing controls. Sequencing and extraction controls are essential for low-biomass microbiota analysis as reagents and tissue handling have been shown to influence the community composition of low-biomass communities (19, 20). In this study, negative extraction

(surgical tools dipped in PBS and then exposed to the same extraction process as tissues, cage bedding, and drinking water) and PCR negative (elution water used instead of the DNA template) samples were included to determine the impact of contaminating DNA. The negative samples were distinct from the nasal tissue microbiota (Fig. S3A) ($P < 0.05$ by PERMANOVA; $R^2 = 0.138$). An unweighted pair group method with arithmetic mean (UPGMA) tree based on Bray-Curtis distances demonstrated the separation between negative controls and samples (Fig. S3B). The dominant taxa in the nasal tissue, namely, *Streptococcus* and *Staphylococcus*, are not present in the negative samples (Fig. S3C). The inclusion of negative samples with every extraction is still worthwhile to distinguish low-abundance communities from reagent contamination.

Mouse source affects the composition of the nasal microbiota. Differences in the murine gut microbiota between breeding sites have been identified as a source of experimental variability (21). We compared the nasal tissue microbiota from mice bred at McMaster University ($n = 32$) to those of mice ordered from Jackson Laboratories (JAX) ($n = 15$). JAX mice have a significantly different nasal microbiota composition compared to in-house-bred mice (Fig. 3A and B) ($P < 0.0001$ by PERMANOVA; $R^2 = 0.226$). While both groups of mice are dominated by *Streptococcaceae*, JAX mice have several other dominant taxa (Fig. 3C). Furthermore, JAX mice had increased α -diversity within the nasal tissue microbiota ($P < 0.001$ by a Mann-Whitney test) (Fig. 4D). LEfSe analysis revealed that 109 genera were significantly different between JAX and in-house-bred mice, including *Mycoplasma* (Fig. 4E) and *Lactobacillus* (Fig. 4F).

***Streptococcus pneumoniae* colonization leads to domination of the nasal microbiota.** *Streptococcus pneumoniae* colonizes the upper respiratory tract, a process which disrupts preexisting microbial communities prior to causing respiratory and invasive infections (9, 10). Investigation into microbial interactions between *S. pneumoniae* and other nasal microbiota members has been primarily performed by analyzing nasal wash samples, which may overlook microbe-microbe interactions occurring deeper in the nasal tissue. Mice were intranasally colonized with *Streptococcus pneumoniae*, and nasal wash and tissue samples were collected after 3 days ($n = 9$ mice). The nasal tissue had higher levels of *S. pneumoniae* than the paired nasal wash sample (Fig. 4A). The cNT and nasal wash microbiota of colonized mice were distinct (Fig. 3B). *S. pneumoniae* dominated the nasal tissue (Fig. 4B and C). LEfSe analysis revealed 24 significantly different genera between the two sampling methods (Fig. S4). Spearman correlations identified that the relative abundance of *Streptococcus* sequence reads strongly correlated with cultured *S. pneumoniae* in the cNT ($R = 0.9$) and nasal wash ($R = 0.95$) samples (Fig. S5). Furthermore, nasal tissue *S. pneumoniae* CFU correlated with nasal wash CFU ($R = 0.95$), and *Streptococcus* amplicon sequence variant (ASV) relative abundances were correlated between nasal tissue and wash samples ($R = 0.88$).

Nasal microbiota correlations are dependent on the tissue extraction methodology. *Staphylococcus* species decrease during *Streptococcus pneumoniae* colonization when sampled by nasal wash (9, 10). *Staphylococcus* and *Streptococcus* species were negatively correlated in the nasal wash samples of *S. pneumoniae*-colonized mice ($R = -0.72$; $P = 0.03$) (Fig. 5A); however, there was no significant correlation for the nasal tissue microbiota ($R = -0.32$; $P = 0.41$) (Fig. 5B). *Corynebacterium* species are overrepresented in the nasal microbiota of children and adults negative for pneumococcal colonization and have recently been identified to inhibit the growth of *S. pneumoniae* *in vitro* (7). No correlation was found between *Corynebacterium* and *Streptococcus* species in the nasal wash microbiota of pneumococcus-colonized mice ($R = 0.36$; $P = 0.35$) (Fig. 5C); however, a strong negative correlation ($R = -0.95$; $P = 8.8 \times 10^{-5}$) between *Corynebacterium* species and *Streptococcus* species existed in the nasal tissue (Fig. 5D), suggesting that interactions between these species could occur within regions not affected by nasal washes. These correlations imply that both sampling techniques may be necessary to uncover microbial interactions that are site specific. Furthermore, niche-specific interactions may be driving antagonism or cooperation between *S. pneumoniae* and other bacterial species in the URT.

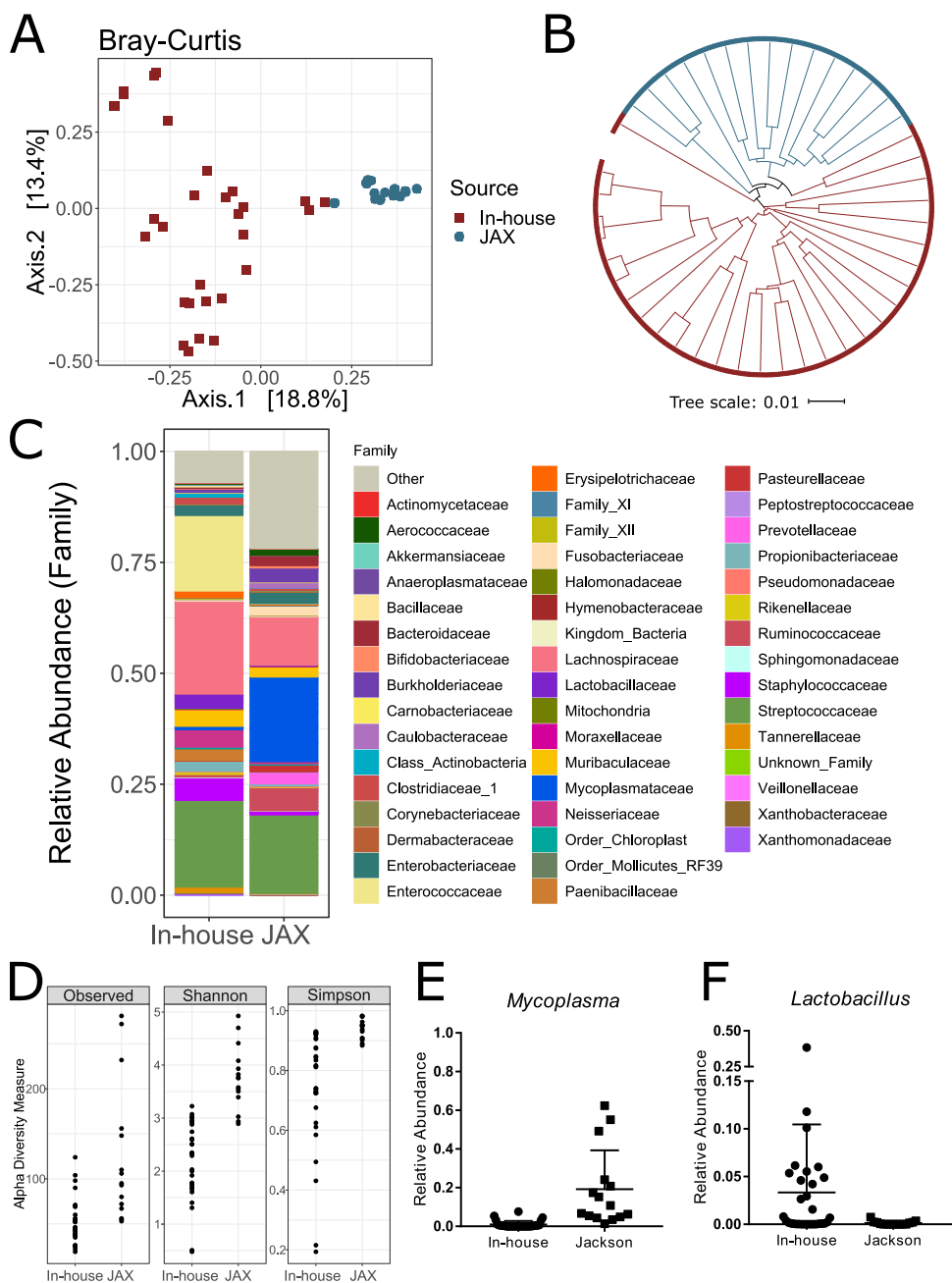


FIG 3 Source of mice impacts nasal microbiota composition. The nasal microbiota of C57BL/6J mice ordered directly from Jackson Laboratories were compared to those of C57BL/6J mice bred in-house for several generations. (A) JAX mice had a significantly distinct microbiota composition ($P < 0.0001$ by PERMANOVA). (B) Bray-Curtis distance tree demonstrating the clustering of mice from Jackson Laboratories compared to mice bred in-house. (C) Taxon summary at the family level comparing the nasal microbiota of in-house-bred mice to those of JAX mice. (D) Alpha-diversity is increased in Jackson Laboratories murine nasal microbiota compared to those of in-house-bred mice, as measured by observed species, Chao1, and Shannon diversity ($P < 0.001$ by a Mann-Whitney test). LEfSe analysis revealed 109 genera within the nasal microbiota that were significantly different between in-house mice and Jackson Laboratories mice. (E and F) The nasal microbiota of mice from Jackson Laboratories were enriched in *Mycoplasma* (E) and decreased in *Lactobacillus* (F) species compared to mice bred in-house.

DISCUSSION

The upper respiratory tract plays an essential role in breathing, trapping inhaled microbes and particles while heating and humidifying air prior to entering the lungs. The topography provides different niches for bacteria to colonize, resulting in protective or

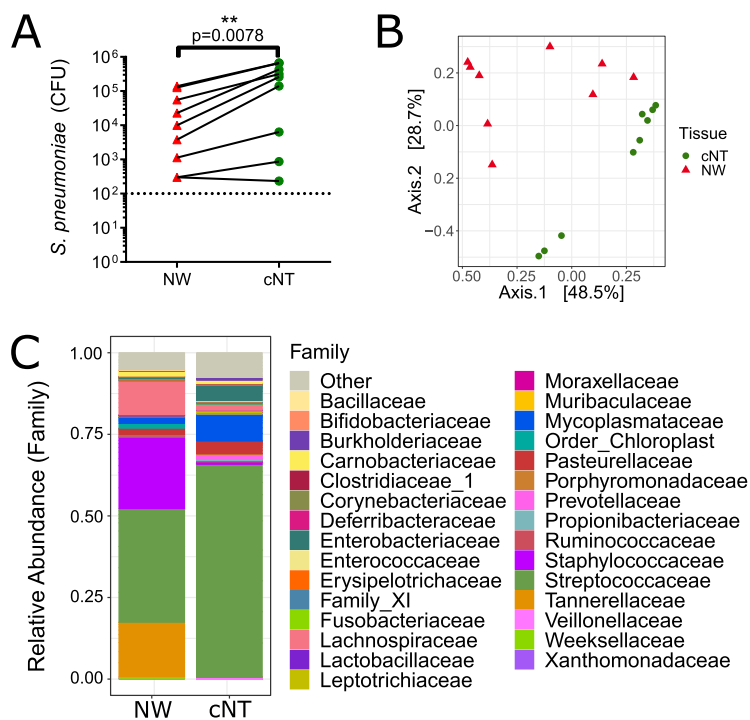


FIG 4 *Streptococcus pneumoniae* dominates the nasal microbiota during colonization. Female C57BL/6J mice were intranasally colonized with 10^7 CFU of *S. pneumoniae* and sacrificed 3 days later for collection of PBS nasal wash samples and complete nasal tissues ($n=9$). (A) Nasal tissue had significantly higher pneumococcal loads than the nasal wash samples ($P=0.0078$ by a Wilcoxon match-paired signed-rank test). (B) The nasal tissue microbiota was distinct from the nasal wash microbiota ($P=0.0002$ by PERMANOVA). (C) Summary taxon plot of the nasal tissue microbiota community (dominated by *Streptococcaceae* and *Mycoplasmataceae*) and the PBS nasal wash microbiota (dominated by *Tannerellaceae*, *Streptococcaceae*, and *Staphylococcaceae*).

deleterious interactions with other microbial species. This study identified that nasal washes do not completely sample the murine nasal microbiota and may overlook some interactions occurring within the turbinates or submucosa of the nasal tissue. Differences in humidity, mucus secretion, and epithelial cell type could contribute to the colonization success of various pathogens and commensals (22, 23). In humans, sampling of different regions of the nasal cavity distinguished the microbial composition of the anterior nares from that of the middle meatus and sphenoidal recess (24). The middle meatus and sphenoidal recess are dominated by *Corynebacterium* and *Staphylococcus* species, while anterior nares have a greater abundance of *Propionibacterium/Cutibacterium* species. In this study, *Actinomyces* and *Neisseria* species were increased in the nasal tissue, whereas the nasal wash samples had greater abundances of *Erysipelotrichaceae* family members. *Actinomyces* and *Neisseria* species in the human nasal microbiota have been associated with an increased risk of acute otitis media.

Select bacterial groups, including *Corynebacterium*, *Staphylococcus*, *Streptococcus*, *Dolosigranulum*, and *Moraxella* species, are commonly found in the human nose (25, 26). The murine nasal microbiota has a dominant *Staphylococcus* and *Streptococcus* population but small *Corynebacterium*, *Dolosigranulum*, and *Moraxella* species populations, similar to mice obtained from Jackson Laboratories and other facilities (9). Mice can be experimentally colonized by *Corynebacterium* and *Moraxella* species, indicating that the low abundance in specific-pathogen-free (SPF) mice could be due to a lack of exposure (27, 28). A major determinant of colonization is adherence, requiring selective interactions between host and bacterial factors. *Neisseria meningitidis* and *Streptococcus pyogenes* colonization in mice requires the expression of human-specific adherence factors in the olfactory epithelium (12, 29).

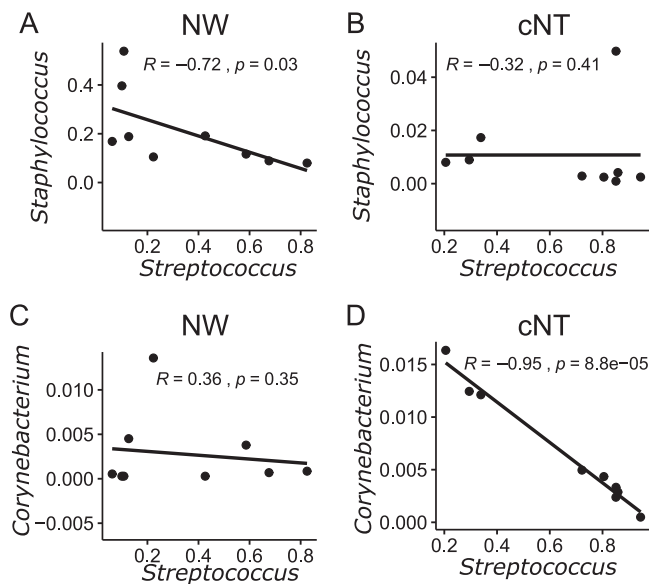


FIG 5 Microbiota interactions depend on the nasal sampling method. Spearman correlations of relative abundances of ASVs in nasal wash samples and nasal tissues of *S. pneumoniae*-colonized mice were determined. (A and B) *Staphylococcus* and *Streptococcus* species have a negative correlation in the PBS nasal wash samples (A) but not nasal tissue (B). (C and D) *Corynebacterium* species have a negative correlation in the nasal tissue (D) but not the nasal wash samples (C). Each dot represents the relative abundance within one animal, from either nasal wash or tissue samples ($n = 9$).

The composition of the microbiota differed between mice bred in-house and those delivered by Jackson Laboratories. Vendor-specific microbiota differences have been identified in gut and lung studies and have been implicated in altering the outcomes of disease models (18, 30, 31); however, our study is the first to demonstrate vendor-specific microbiome differences within the nasal tissue. Housing under SPF conditions at different facilities restricts access to many bacteria beyond pathogens, and SPF mice have drastically different respiratory microbiota compositions compared to wild mice (32). Indeed, mice captured from the wild have more, as well as different, bacteria in their lungs, which influences alveolar structure (32). The impact of differential colonization between facilities and sources may impact the baseline physiology or expression of some genes. Krone et al. previously assessed the murine nasal microbiota by nasal wash and found patterns similar to those in our mice, with high levels of *Staphylococcaceae*, *Streptococcaceae*, and *Erysipelotrichaceae*, but failed to detect *Actinomycetaceae* (9), which were detected in the nasal tissue samples in this study. Interestingly, Weyrich et al. found high levels of *Actinomycetaceae* (as well as *Streptococcaceae* and *Staphylococcaceae*) in nasal tissue samples from their facility (33). Whether these differences are due to different breeding facilities, housing conditions, or sampling techniques is unclear.

Sequencing-based analysis of the URT microbiota is complicated due to the low microbial biomass compared to host DNA (34). Extraction and amplification methods will affect the outcome of sequencing results, and the inclusion of template negative controls is essential for determination of the microbial composition. We demonstrated that the nasal tissue microbiota is distinct from the gut microbiota and negative controls. Furthermore, there was a strong correlation between the cultivable amount of inoculated *S. pneumoniae* and the ability to detect *Streptococcus* ASVs in the nasal tissue and wash samples. This strongly suggests that culture-independent analysis of the nasal tissue microbiota is representative of the cultivable microbiota and not contaminating DNA sequences from environmental or extraction sources.

Colonization is essential during bacterial pathogenesis, including adherence prior to invasion or spread to new hosts. Capsule expression by *Streptococcus pneumoniae*

varies depending on nasal location, which alters its ability to adhere, evade killing, or be transmitted to a new host (35–38). As such, the detection of *S. pneumoniae* in nasal wash or tissue extraction samples has different implications for transmission versus invasive disease. Multiple studies have reported a negative correlation between *Staphylococcus* and *Streptococcus* species, potentially due to hydrogen peroxide production (39, 40). We have shown that this negative correlation exists in the nasopharynx of colonized mice but not in the nasal tissue. Conversely, we have shown a negative correlation between *Streptococcus* and *Corynebacterium* species in the nasal tissue but not in the nasal wash samples. *Corynebacterium* species have been demonstrated to liberate host triacylglycerols that kill *S. pneumoniae* (7). Previous studies have also implicated differences in *Haemophilus influenzae* and *S. pneumoniae* antagonism depending on the sampling method (15, 16). Together, these data suggest that multiple sampling methods may be necessary to determine bacterial interactions within the URT. Human experimental colonization models assess pneumococcal colonization, as well as microbial communities, via nasal wash (41) and identify many antagonistic interactions that have also been seen in murine models of experimental colonization (e.g., negative correlation of *Corynebacterium* and *Streptococcus* [41, 42]); however, whether there are microbial interactions missed by this sampling method is unclear. The structure of murine nasal tissue is much more complicated than that of human nasal tissue, so species-specific sampling techniques may be needed to study microbial interactions.

Overall, mechanistic investigation of the URT microbiota in infection and immunity requires animal models. Current studies have used mixed methodologies, including different sampling techniques and mouse vendors, to investigate development and disease phenotypes. Proper extraction and assessment of the nasal tissue of mice are essential to reveal reproducible, mechanistic interactions between host cells and microbial members. Our findings demonstrate that assessment of the nasal microbiota is dependent on biogeography and needs to be integrated into research design for evaluation of pathogen and commensal colonization and interactions.

MATERIALS AND METHODS

Animals. C57Bl/6J mice were bred within the McMaster Central Animal Facility, except for the experiments in which we used female C57Bl/6J mice from Jackson Laboratories (Bar Harbor, ME). Mice from Jackson Labs were 6 to 8 weeks old and acclimated to specific pathogen-free conditions for 2 weeks prior to experiments. All mice had access to food and water *ad libitum*. All mice used in this study were female mice aged 8 to 12 weeks. Mice were anesthetized using isoflurane and euthanized by exsanguination. All experiments were approved by McMaster University's Animal Research Ethics Board according to the recommendations of the Canadian Council for Animal Care.

Tissue collection. Nasal wash was completed as previously described (43). Briefly, a PE-20 polyethylene tube attached to a 26-gauge needle was inserted through a small incision in the trachea. Lavages were performed with 300 μ l of sterilized phosphate-buffered saline (PBS) or buffer RLT (Qiagen), which was flushed through the trachea and collected through the nares in a 1.7-ml microtube. Complete nasal tissue (cNT) was collected from lavaged or naive mice via bisection of the skull with sterilized surgical tools (44). Excised tissues were homogenized in 300 μ l PBS in 2-ml screw-top tubes using 2.8-mm ceramic beads for 1 min at 2,000 rpm (MoBio).

Histological analysis. After nasal washes, mouse heads were placed into formalin for 24 h before being placed in a Shandon TBD-2 decalcifier (Thermo Scientific, Kalamazoo, MI) for 4 days. Decalcified heads were placed in formalin for 2 days, followed by twice-daily washes with PBS for an additional 4 days. Samples were washed with and placed in 70% ethanol prior to standard histological processing and embedded in paraffin wax. Cross-sectional slices (5 μ m) were mounted on slides and stained with hematoxylin and eosin according to standard protocols. Slides were randomized and scored in a blind fashion. The integrity of the epithelial lining was measured by quantifying the area of intact/disrupted epithelium using ImageJ.

DNA extraction, amplification, and analysis of the 16S rRNA gene. DNA was extracted from PBS nasal wash and cNT homogenates as previously described (10). Samples were mechanically homogenized with 0.2 g of 0.1-mm glass beads and 0.2 g of 2.8-mm glass beads in 800 μ l of 200 mM NaPO₄ (pH 8) and 100 μ l of guanidine thiocyanate-EDTA-*N*-lauroyl sarcosine. After homogenization, the sample was incubated with 50 μ l of lysozyme (100 mg/ml) and 10 μ l of RNase A (10 mg/ml) for 1 h at 37°C, followed by incubation with a solution containing 25 μ l sodium dodecyl sulfate (25%), 62.5 μ l NaCl (5 M), and 25 μ l proteinase K (20 mg/ml) for 1 h at 65°C. Samples were centrifuged for 5 min at maximum speed, and the supernatant was transferred to 900 μ l of buffered phenol-chloroform-isomyl alcohol (25:24:1). Samples were vortexed and centrifuged for 10 min at maximum speed prior to

transferring the aqueous phase to DNA Clean and Concentrator-25 columns (Zymo) according to the manufacturer's instructions, except that samples were eluted with 50 μ l ultrapure water. Negative controls included PBS-exposed surgical tools, cage bedding, drinking water, and no-template PCR amplicons.

PCR amplification of the 16S rRNA gene (V3 region) involved a two-step, nested PCR, which improves efficiency in the presence of high host DNA levels (45). The first step involved the amplification of the 16S rRNA gene region spanning V1 to V5 using universal primers 8F (AGAGTTTGATCCTGGCTCAG) and 926R (CCGTCAATTCCTTTRAGTTT) for 15 cycles (94°C for 30 s, 56°C for 30 s, and 72°C for 60 s). This product was used as the template in the second reaction for 25 cycles (94°C for 30 s, 47°C for 30 s, and 72°C for 40 s) to amplify the V3 region of the 16S rRNA gene in preparation for MiSeq (Illumina) sequencing. Barcoded primer sequences were adapted similarly to previous work (46). All reactions, including extraction negative and no-template controls, were performed in triplicate to reduce PCR bias, and reaction mixtures were pooled prior to sequencing using the MiSeq sequencing platform (Illumina, Inc., San Diego, CA) at the Farncombe Genomics Facility at McMaster University. Sequences were trimmed using CutAdapt (47) prior to analysis with DADA2 (48) to organize sequences into amplicon sequence variants (ASVs). Taxonomy was assigned using the Silva database (49). Relative abundance, α - and β -diversity, and rarefactions were completed using the Phyloseq package (50) in R version 3.5.2 (51). A dendrogram was constructed based on unweighted pair group method with arithmetic mean (UPGMA) hierarchical clustering using Bray-Curtis distances using the phangorn package (52) and plotted with iTOL (53). Differences between bacterial communities were tested using permutational multivariate analysis of variance (PERMANOVA) within the vegan package (54). Differences in taxon abundances were assessed using linear discriminant analysis (LDA) effect size (LEfSe) (55).

Streptococcus pneumoniae colonization. Mice were intranasally colonized with *S. pneumoniae* strain P1547 (serotype 6A), obtained from Jeff Weiser (NYU School of Medicine), as previously described (43). *S. pneumoniae* was grown in tryptic soy broth in a 5% CO₂ incubator at 37°C until cultures were in late log phase (optical density at 600 nm [OD₆₀₀] = 0.5). Cultures were spun down at 15,000 \times g for 1 min and resuspended at a concentration of 10⁹ CFU/ml in PBS. Mice were colonized by depositing 10 μ l containing 10⁷ CFU of *S. pneumoniae* directly in the nares. Mice were sacrificed at 3 days postinoculation prior to PBS nasal wash and cNT sample collection.

Bacterial culture. PBS nasal wash and tissue homogenates were incubated overnight on brain heart infusion agar or tryptic soy agar supplemented with 5% sheep's blood and neomycin (10 μ g/ml) or on pre-reduced fastidious anaerobic agar in an anaerobic chamber. Colonies were counted and collected via the addition of 1 ml BHI medium and scraping the plate surface with a cell scraper. A portion of the collected colonies was frozen at -80°C in 10% glycerol, while the remainder was prepared for genomic extraction.

Statistical analysis. GraphPad Prism 6 and R were used for statistical analysis. Nonparametric tests were used for comparison of histology scoring and bacterial plate counts. Differences with *P* values of <0.05 were considered statistically significant. Microbial community composition differences were determined using the Adonis function (PERMANOVA) with 10,000 permutations.

Data availability. Data related to this study have been deposited in the NCBI database under BioProject accession number [PRJNA679949](https://www.ncbi.nlm.nih.gov/bioproject/PRJNA679949).

SUPPLEMENTAL MATERIAL

Supplemental material is available online only.

FIG S1, TIF file, 0.04 MB.

FIG S2, EPS file, 0.2 MB.

FIG S3, EPS file, 0.2 MB.

FIG S4, EPS file, 0.3 MB.

FIG S5, EPS file, 0.3 MB.

FIG S6, EPS file, 0.2 MB.

ACKNOWLEDGMENTS

L.P.S. was supported by a scholarship from the Canadian Institutes of Health Research (CIHR). This work was funded by grants from the CIHR to D.M.E.B. and M.G.S. D.M.E.B. and M.G.S. are supported by the CIHR and hold Canada Research Chairs, with further support from the McMaster Immunology Research Centre and the Michael G. Degroote Institute for Infectious Disease Research.

We thank Laura Rossi, Michelle Shah, and the Farncombe Metagenomic facility for DNA sequencing assistance.

REFERENCES

- Bogaert D, De Groot R, Hermans PWM. 2004. Streptococcus pneumoniae colonisation: the key to pneumococcal disease. *Lancet Infect Dis* 4:144–154. [https://doi.org/10.1016/S1473-3099\(04\)00938-7](https://doi.org/10.1016/S1473-3099(04)00938-7).
- Bogaert D, van Belkum A, Sluiter M, Luijendijk A, de Groot R, Rümke HC, Verbrugh HA, Hermans PWM. 2004. Colonisation by Streptococcus pneumoniae and Staphylococcus aureus in healthy children. *Lancet* 363:1871–1872. [https://doi.org/10.1016/S0140-6736\(04\)16357-5](https://doi.org/10.1016/S0140-6736(04)16357-5).
- Regev-Yochay G, Dagan R, Raz M, Carmeli Y, Shainberg B, Derazne E, Rahav

- G, Rubinstein E. 2004. Association between carriage of *Streptococcus pneumoniae* and *Staphylococcus aureus* in children. *JAMA* 292:716–720. <https://doi.org/10.1001/jama.292.6.716>.
4. Bosch AATM, van Houten MA, Bruin JP, Wijmenga-Monsuur AJ, Trzciński K, Bogaert D, Rots NY, Sanders EAM. 2016. Nasopharyngeal carriage of *Streptococcus pneumoniae* and other bacteria in the 7th year after implementation of the pneumococcal conjugate vaccine in the Netherlands. *Vaccine* 34:531–539. <https://doi.org/10.1016/j.vaccine.2015.11.060>.
 5. Biesbroek G, Tsvitvadze E, Sanders EAM, Montijn R, Veenhoven RH, Keijsers BJF, Bogaert D. 2014. Early respiratory microbiota composition determines bacterial succession patterns and respiratory health in children. *Am J Respir Crit Care Med* 190:1283–1292. <https://doi.org/10.1164/rccm.201407-12400C>.
 6. Hardy BL, Dickey SW, Plaut RD, Riggins DP, Stibitz S, Otto M, Merrell DS. 2019. *Corynebacterium pseudodiphtheriticum* exploits *Staphylococcus aureus* virulence components in a novel polymicrobial defense strategy. *mBio* 10:e02491-18. <https://doi.org/10.1128/mBio.02491-18>.
 7. Bomar L, Brugger SD, Yost BH, Davies SS, Lemon KP. 2016. *Corynebacterium accolens* releases antipneumococcal free fatty acids from human nostril and skin surface triacylglycerols. *mBio* 7:e01725-15. <https://doi.org/10.1128/mBio.01725-15>.
 8. Cremers AJ, Zomer AL, Gritzfeld JF, Ferwerda G, van Hijum SA, Ferreira DM, Shak JR, Klugman KP, Boekhorst J, Timmerman HM, de Jonge MI, Gordon SB, Hermans PW. 2014. The adult nasopharyngeal microbiome as a determinant of pneumococcal acquisition. *Microbiome* 2:44. <https://doi.org/10.1186/2049-2618-2-44>.
 9. Krone CL, Biesbroek G, Trzciński K, Sanders EAM, Bogaert D. 2014. Respiratory microbiota dynamics following *Streptococcus pneumoniae* acquisition in young and elderly mice. *Infect Immun* 82:1725–1731. <https://doi.org/10.1128/IAI.01290-13>.
 10. Thevaranjan N, Whelan FJ, Puchta A, Ashu E, Rossi L, Surette MG, Bowdish DME. 2016. *Streptococcus pneumoniae* colonization disrupts the microbial community within the upper respiratory tract of aging mice. *Infect Immun* 84:906–916. <https://doi.org/10.1128/IAI.01275-15>.
 11. Owen SJ, Batzloff M, Chehrehasa F, Meedeniya A, Casart Y, Logue C, Hirst RG, Peak IR, Mackay-Sim A, Beacham IR. 2009. Nasal-associated lymphoid tissue and olfactory epithelium as portals of entry for *Burkholderia pseudomallei* in murine melioidosis. *J Infect Dis* 199:1761–1770. <https://doi.org/10.1086/599210>.
 12. Kasper KJ, Zeppa JJ, Wakabayashi AT, Xu SX, Mazzuca DM, Welch I, Baroja ML, Kotb M, Cairns E, Cleary PP, Haeryfar SMM, McCormick JK. 2014. Bacterial superantigens promote acute nasopharyngeal infection by *Streptococcus pyogenes* in a human MHC class II-dependent manner. *PLoS Pathog* 10:e1004155. <https://doi.org/10.1371/journal.ppat.1004155>.
 13. Meyer Sauter PM, de Groot RCA, Estevão SC, Hoogenboezem T, de Buijn ACJM, Sluijter M, de Buijn MJW, De Kleer IM, van Haperen R, van den Brand JMA, Bogaert D, Fraaij PLA, Vink C, Hendriks RW, Samsom JN, Ungar WWJ, van Rossum AMC. 2018. The role of B cells in carriage and clearance of *Mycoplasma pneumoniae* from the respiratory tract of mice. *J Infect Dis* 217:298–309. <https://doi.org/10.1093/infdis/jix559>.
 14. Liang B, Hyland L, Hou S. 2001. Nasal-associated lymphoid tissue is a site of long-term virus-specific antibody production following respiratory virus infection of mice. *J Virol* 75:5416–5420. <https://doi.org/10.1128/JVI.75.11.5416-5420.2001>.
 15. Lysenko ES, Ratner AJ, Nelson AL, Weiser JN. 2005. The role of innate immune responses in the outcome of interspecies competition for colonization of mucosal surfaces. *PLoS Pathog* 1:e1. <https://doi.org/10.1371/journal.ppat.0010001>.
 16. Margolis E, Yates A, Levin BR. 2010. The ecology of nasal colonization of *Streptococcus pneumoniae*, *Haemophilus influenzae* and *Staphylococcus aureus*: the role of competition and interactions with host's immune response. *BMC Microbiol* 10:59. <https://doi.org/10.1186/1471-2180-10-59>.
 17. Briles DE, Novak L, Hotomi M, van Ginkel FW, King J. 2005. Nasal colonization with *Streptococcus pneumoniae* includes subpopulations of surface and invasive pneumococci. *Infect Immun* 73:6945–6951. <https://doi.org/10.1128/IAI.73.10.6945-6951.2005>.
 18. Dickson RP, Erb-Downward JR, Falkowski NR, Hunter EM, Ashley SL, Huffnagle GB. 2018. The lung microbiota of healthy mice are highly variable, cluster by environment, and reflect variation in baseline lung innate immunity. *Am J Respir Crit Care Med* 198:497–508. <https://doi.org/10.1164/rccm.201711-21800C>.
 19. de Goffau MC, Lager S, Salter SJ, Wagner J, Kronbichler A, Charnock-Jones DS, Peacock SJ, Smith GCS, Parkhill J. 2018. Recognizing the reagent microbiome. *Nat Microbiol* 3:851–853. <https://doi.org/10.1038/s41564-018-0202-y>.
 20. Salter SJ, Cox MJ, Turek EM, Calus ST, Cookson WO, Moffatt MF, Turner P, Parkhill J, Loman NJ, Walker AW. 2014. Reagent and laboratory contamination can critically impact sequence-based microbiome analyses. *BMC Biol* 12:87. <https://doi.org/10.1186/s12915-014-0087-z>.
 21. Alegre ML. 2019. Mouse microbiomes: overlooked culprits of experimental variability. *Genome Biol* 20:108. <https://doi.org/10.1186/s13059-019-1723-2>.
 22. Rigottier-Gois L. 2013. Dysbiosis in inflammatory bowel diseases: the oxygen hypothesis. *ISME J* 7:1256–1261. <https://doi.org/10.1038/ismej.2013.80>.
 23. Siegel SJ, Weiser JN. 2015. Mechanisms of bacterial colonization of the respiratory tract. *Annu Rev Microbiol* 69:425–444. <https://doi.org/10.1146/annurev-micro-091014-104209>.
 24. Yan M, Pamp SJ, Fukuyama J, Hwang PH, Cho DY, Holmes S, Relman DA. 2013. Nasal microenvironments and interspecific interactions influence nasal microbiota complexity and *S. aureus* carriage. *Cell Host Microbe* 14:631–640. <https://doi.org/10.1016/j.chom.2013.11.005>.
 25. Biesbroek G, Bosch AATM, Wang X, Keijsers BJF, Veenhoven RH, Sanders EAM, Bogaert D. 2014. The impact of breastfeeding on nasopharyngeal microbial communities in infants. *Am J Respir Crit Care Med* 190:298–308. <https://doi.org/10.1164/rccm.201401-00730C>.
 26. Stearns JC, Davidson CJ, McKeon S, Hwang J, Fontes ME, Schryvers AB, Bowdish DME, Kellner JD, Surette MG. 2015. Culture and molecular-based profiles show shifts in bacterial communities of the upper respiratory tract that occur with age. *ISME J* 9:1246–1259. <https://doi.org/10.1038/ismej.2014.250>.
 27. Abreu NA, Nagalingam NA, Song Y, Roediger FC, Pletcher SD, Goldberg AN, Lynch SV. 2012. Sinus microbiome diversity depletion and *Corynebacterium tuberculo-stearicum* enrichment mediates rhinosinusitis. *Sci Transl Med* 4:151ra124. <https://doi.org/10.1126/scitranslmed.3003783>.
 28. Krishnamurthy A, McGrath J, Cripps AW, Kyd JM. 2009. The incidence of *Streptococcus pneumoniae* otitis media is affected by the polymicrobial environment particularly *Moraxella catarrhalis* in a mouse nasal colonisation model. *Microbes Infect* 11:545–553. <https://doi.org/10.1016/j.micinf.2009.03.001>.
 29. Johswich KO, McCaw SE, Islam E, Sintsova A, Gu A, Shively JE, Gray-Owen SD. 2013. In vivo adaptation and persistence of *Neisseria meningitidis* within the nasopharyngeal mucosa. *PLoS Pathog* 9:e1003509. <https://doi.org/10.1371/journal.ppat.1003509>.
 30. Velazquez EM, Nguyen H, Heasley KT, Saechao CH, Gil LM, Rogers AWL, Miller BM, Rolston MR, Lopez CA, Litvak Y, Liou MJ, Faber F, Bronner DN, Tiffany CR, Byndloss MX, Byndloss AJ, Bäumlner AJ. 2019. Endogenous Enterobacteriaceae underlie variation in susceptibility to *Salmonella* infection. *Nat Microbiol* 4:1057–1064. <https://doi.org/10.1038/s41564-019-0407-8>.
 31. Ivanov II, Frutos RDL, Manel N, Yoshinaga K, Rifkin DB, Sartor RB, Finlay BB, Littman DR. 2008. Specific microbiota direct the differentiation of IL-17-producing T-helper cells in the mucosa of the small intestine. *Cell Host Microbe* 4:337–349. <https://doi.org/10.1016/j.chom.2008.09.009>.
 32. Yun Y, Srinivas G, Kuenzel S, Linnenbrink M, Alnahas S, Bruce KD, Steinhoff U, Baines JF, Schaible UE. 2014. Environmentally determined differences in the murine lung microbiota and their relation to alveolar architecture. *PLoS One* 9:e0113466. <https://doi.org/10.1371/journal.pone.0113466>.
 33. Weyrich LS, Feaga HA, Park J, Muse SJ, Safi CY, Rolin OY, Young SE, Harvill ET. 2014. Resident microbiota affect *Bordetella pertussis* infectious dose and host specificity. *J Infect Dis* 209:913–921. <https://doi.org/10.1093/infdis/jit597>.
 34. Yu G, Fadrosch D, Goedert JJ, Ravel J, Goldstein AM. 2015. Nested PCR biases in interpreting microbial community structure in 16S rRNA gene sequence datasets. *PLoS One* 10:e0132253. <https://doi.org/10.1371/journal.pone.0132253>.
 35. Cundell DR, Gerard NP, Gerard C, Idanpaan-Heikkilä I, Tuomanen EI. 1995. *Streptococcus pneumoniae* anchor to activated human cells by the receptor for platelet-activating factor. *Nature* 377:435–438. <https://doi.org/10.1038/377435a0>.
 36. Kietzman CC, Gao G, Mann B, Myers L, Tuomanen EI. 2016. Dynamic capsule restructuring by the main pneumococcal autolysin *LytA* in response to the epithelium. *Nat Commun* 7:10859. <https://doi.org/10.1038/ncomms10859>.
 37. Weiser JN, Bae D, Epino H, Gordon SB, Kapoor M, Zenewicz LA, Shchepetov M. 2001. Changes in availability of oxygen accentuate differences in capsular polysaccharide expression by phenotypic variants and clinical isolates

- of *Streptococcus pneumoniae*. *Infect Immun* 69:5430–5439. <https://doi.org/10.1128/iai.69.9.5430-5439.2001>.
38. Weiser JN, Austrian R, Sreenivasan PK, Masure HR. 1994. Phase variation in pneumococcal opacity: relationship between colonial morphology and nasopharyngeal colonization. *Infect Immun* 62:2582–2589. <https://doi.org/10.1128/IAI.62.6.2582-2589.1994>.
 39. Quintero B, Araque M, van der Gaast-de Jongh C, Escalona F, Correa M, Morillo-Puente S, Vielma S, Hermans PWM. 2011. Epidemiology of *Streptococcus pneumoniae* and *Staphylococcus aureus* colonization in healthy Venezuelan children. *Eur J Clin Microbiol Infect Dis* 30:7–19. <https://doi.org/10.1007/s10096-010-1044-6>.
 40. Regev-Yochay G, Trzcinski K, Thompson CM, Malley R, Lipsitch M. 2006. Interference between *Streptococcus pneumoniae* and *Staphylococcus aureus*: in vitro hydrogen peroxide-mediated killing by *Streptococcus pneumoniae*. *J Bacteriol* 188:4996–5001. <https://doi.org/10.1128/JB.00317-06>.
 41. de Steenhuijsen P, WAA, Jochems SP, Mitsi E, Rylance J, Pojar S, Nikolaou E, German EL, Holloway M, Carniel BF, Chu MLJN, Arp K, Sanders EAM, Ferreira DM, Bogaert D. 2019. Interaction between the nasal microbiota and *S. pneumoniae* in the context of live-attenuated influenza vaccine. *Nat Commun* 10:2981. <https://doi.org/10.1038/s41467-019-10814-9>.
 42. Kelly MS, Surette MG, Smieja M, Rossi L, Luinstra K, Steenhoff AP, Goldfarb DM, Pernica JM, Arscott-Mills T, Boiditswe S, Mazhani T, Rawls JF, Cunningham CK, Shah SS, Feemster KA, Seed PC. 2018. Pneumococcal colonization and the nasopharyngeal microbiota of children in Botswana. *Pediatr Infect Dis J* 37:1176–1183. <https://doi.org/10.1097/INF.0000000000002174>.
 43. Puchta A, Verschoor CP, Thurn T, Bowdish DME. 2014. Characterization of inflammatory responses during intranasal colonization with *Streptococcus pneumoniae*. *J Vis Exp* 2014:e50490. <https://doi.org/10.3791/50490>.
 44. Zeppa JJ, Wakabayashi AT, Kasper KJ, Xu SX, Haeryfar SMM, McCormick JK. 2016. Nasopharyngeal infection of mice with *Streptococcus pyogenes* and in vivo detection of superantigen activity. *Methods Mol Biol* 1396:95–107. https://doi.org/10.1007/978-1-4939-3344-0_8.
 45. Stearns JC, Lynch MDJ, Senadheera DB, Tenenbaum HC, Goldberg MB, Cvitkovich DG, Croitoru K, Moreno-Hagelsieb G, Neufeld JD. 2011. Bacterial biogeography of the human digestive tract. *Sci Rep* 1:170. <https://doi.org/10.1038/srep00170>.
 46. Bartram AK, Lynch MDJ, Stearns JC, Moreno-Hagelsieb G, Neufeld JD. 2011. Generation of multimillion-sequence 16S rRNA gene libraries from complex microbial communities by assembling paired-end Illumina reads. *Appl Environ Microbiol* 77:3846–3852. <https://doi.org/10.1128/AEM.02772-10>.
 47. Martin M. 2011. Cutadapt removes adapter sequences from high-throughput sequencing reads. *EMBnet J* 17:10–12. <https://doi.org/10.14806/ej.17.1.200>.
 48. Callahan BJ, McMurdie PJ, Rosen MJ, Han AW, Johnson AJA, Holmes SP. 2016. DADA2: high-resolution sample inference from Illumina amplicon data. *Nat Methods* 13:581–583. <https://doi.org/10.1038/nmeth.3869>.
 49. Quast C, Pruesse E, Yilmaz P, Gerken J, Schweer T, Yarza P, Peplies J, Glöckner FO. 2013. The SILVA ribosomal RNA gene database project: improved data processing and Web-based tools. *Nucleic Acids Res* 41: D590–D596. <https://doi.org/10.1093/nar/gks1219>.
 50. McMurdie PJ, Holmes S. 2013. phyloseq: an R package for reproducible interactive analysis and graphics of microbiome census data. *PLoS One* 8: e61217. <https://doi.org/10.1371/journal.pone.0061217>.
 51. R Core Team. 2018. R: a language and environment for statistical computing. R Foundation for Statistical Computing, Vienna, Austria.
 52. Schliep KP. 2011. phangorn: phylogenetic analysis in R. *Bioinformatics* 27:592–593. <https://doi.org/10.1093/bioinformatics/btq706>.
 53. Letunic I, Bork P. 2016. Interactive Tree of Life (iTOL) v3: an online tool for the display and annotation of phylogenetic and other trees. *Nucleic Acids Res* 44:W242–W245. <https://doi.org/10.1093/nar/gkw290>.
 54. Oksanen J, Blanchet FG, Friendly M, Roeland K, Legendre P, McGlenn D, Minchin PR, O'Hara RB, Simpson GL, Solymos P, Stevens MHH, Szoecs E, Wagner H. 2019. vegan: community ecology package. R package version 2.5-4.
 55. Segata N, Izard J, Waldron L, Gevers D, Miropolsky L, Garrett WS, Huttenhower C. 2011. Metagenomic biomarker discovery and explanation. *Genome Biol* 12: R60. <https://doi.org/10.1186/gb-2011-12-6-r60>.